

Concerning the Circular- and Square-loop Antennas Mounted over a Ground Plane of Finite Extent

A. A. Ayorinde¹, S. A. Adekola^{1,2}, and A. Ike Mowete¹

¹Department of Electrical and Electronics Engineering
Faculty of Engineering, University of Lagos, Lagos, Nigeria

²Department of Electrical and Electronics Engineering
Niger Delta University, Wilberforce Island, Yenegoa, Nigeria

Abstract— As a natural sequel to an earlier presentation [1], which compared the performance features of equal perimeter circular- and square-loop antennas located over finite ground planes, this paper, using the same formulation, examines the same performance characteristics, but this time, with the antennas being of equal cross-sectional areas; and with loop heights varying between 0.05λ and 1.00λ at the operating (center) frequency of 1.25 GHz. Computational results for the antennas' input characteristics reveal that whereas they share virtually identical input resistance profiles, input reactance for the square loop has values that are in general, lower than those for the circular loop, for the entire range of 'height above ground plane' considered. Results for the E - and H -plane radiation field patterns indicate that when the loops are located at heights beyond 0.3λ above the finite ground plane, the front-lobes become distorted; an observation supported by the profiles of the forward directive gain, which display the 'notch filter response' behavior. Furthermore, the results suggest that acceptable front-to-back ratio performance can only be maintained if loop heights above the ground plane are kept below 0.3λ .

1. INTRODUCTION

The transformation of the characteristic bidirectional field pattern of a loop antenna radiating in free space to a unidirectional pattern is traditionally accomplished by backing the loop antenna with a large ground plane [6]. A typical example of an analytical technique employed for such structures is provided by the work of Shoamanesh and Shafai (1981) [5], in which the ground plane is considered as being essentially of infinite extent, (so that the image theory applies) and where analytical results reported a consequent gain enhancement for the antenna. The more practical problem for which the ground plane is of finite extent is more demanding because apart from the geometrical field and the reflected field that require evaluation, the diffracted fields due to the ground plane's edges must also be fully accounted for.

Previous notable works on the loop antenna located above a finite ground plane include that reported by Rojarajamont and Sekiguichi [2] who used an approximate current on the finite ground plane deduced from current due an infinite ground plane. Iwashige [3] employed the equivalent edge currents technique to evaluate the diffraction fields of a circular reflector, whereas Hejase et al. [4] utilized the Physical Optics (PO) method to determine the induced current on the square plate backing a circular loop antenna. In an earlier presentation, Ayorinde et al. [1] replaced the finite (solid) ground plane by grids constructed with thin wires, to address the radiation field problems of the circular-loop and square-loop antennas located above finite ground plane.

As an extension of that effort [1], this presentation examines the performance characteristics of circular- and square-loop antennas located over wire-grid ground planes of finite extent, with both loops characterized by equal cross-sectional areas. In addition to input impedance, far-zone fields and associated directive gain features; the front-to-back ratio (F/B) of the radiation intensity is also given consideration in this paper. And computational results suggest that for both loop antenna geometries of interest, an acceptable front-to-back ratio performance is sustainable when the antenna heights above the ground plane are less than 0.3λ at the operating frequency.

2. FORMULATION

Displayed in Figure 1(a) is a thin-wire circular loop antenna mounted at height h above a wire-grid ground plane while Figure 1(b) depicts a thin-wire square loop antenna at height h over a ground plane modeled by wire grids. It should be remarked that the above problem geometries are similar to the geometry studied in [1]. However, our interest here is when the cross-sectional area of the circular loop is equal to that of the square loop, that is, $[\pi a^2 = b^2]$, unlike in previous presentation [1], where the two loops have equal perimeter. Because the grids are constructed with

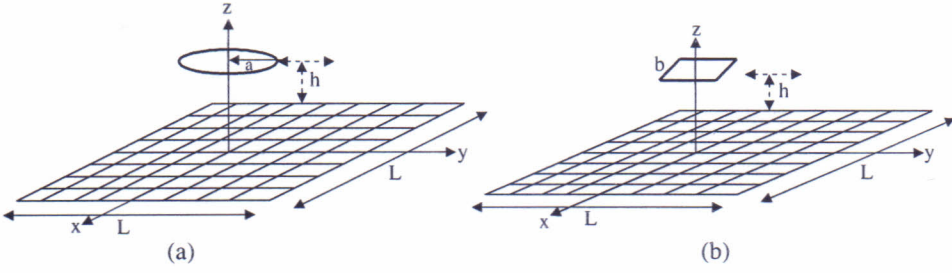


Figure 1: (a) A circular-loop antenna of radius a suspended at height h from a wire-grid ground plane. (b) A square loop antenna of side-length b at height h above a wire-grid ground plane.

both x -directed and y -directed wires, the total electric field at the far-zone is the superposition of the electric fields from the loop as well as the x -directed and y -directed wires. To avoid undue repetition, we rely substantially on the theory developed in [1], and therefore E_θ and E_φ components of the far-zone fields assume the following expressions:

$$E_\theta = E_{\ell\theta} + \sum_{n=1}^N E_{n\theta}^x + \sum_{n=1}^N E_{n\theta}^y \quad (1a)$$

and

$$E_\varphi = E_{\ell\varphi} + \sum_{n=1}^N E_{n\varphi}^x + \sum_{n=1}^N E_{n\varphi}^y \quad (1b)$$

where $E_{\ell\theta}$, $E_{n\theta}^x$ and $E_{n\theta}^y$ are the \hat{a}_θ -components of the electric fields due axial current distributions along the loop, n th x -directed wires and n th y -directed wires, respectively; while $E_{\ell\varphi}$, $E_{n\varphi}^x$ and $E_{n\varphi}^y$ are the \hat{a}_φ -components of the electric fields due to respective axial currents on the loop, n th x -directed and n th y -directed wires. The above electric field components can be calculated from:

$$E_{n\theta}^x = \frac{-j\omega\mu_0 e^{-jk_0 r} \cos\theta \cos\varphi}{4\pi r} \int_{-L/2}^{L/2} I(x') e^{jk_0 [x' \cos\varphi \sin\theta + (n-5)\frac{\lambda}{8} \sin\varphi \sin\theta]} dx' \quad (2a)$$

$$E_{n\theta}^y = \frac{-j\omega\mu_0 e^{-jk_0 r} \cos\theta \sin\varphi}{4\pi r} \int_{-L/2}^{L/2} I(y') e^{jk_0 [y' \sin\varphi \sin\theta + (n-5)\frac{\lambda}{8} \cos\varphi \sin\theta]} dy' \quad (2b)$$

$$E_{n\varphi}^x = \frac{j\omega\mu_0 e^{-jk_0 r} \sin\varphi}{4\pi r} \int_{-L/2}^{L/2} I(x') e^{jk_0 [x' \cos\varphi \sin\theta + (n-5)\frac{\lambda}{8} \sin\varphi \sin\theta]} dx' \quad (3a)$$

$$E_{n\varphi}^y = \frac{-j\omega\mu_0 e^{-jk_0 r} \cos\varphi}{4\pi r} \int_{-L/2}^{L/2} I(y') e^{jk_0 [y' \sin\varphi \sin\theta + (n-5)\frac{\lambda}{8} \cos\varphi \sin\theta]} dy' \quad (3b)$$

for circular loop $\ell = c$

$$E_{c\theta} = \frac{-j\omega\mu_0 a e^{-jk_0 r} \cos\theta}{4\pi r} \int_0^{2\pi} \sin(\varphi - \varphi') I(\varphi') e^{jk_0 [a \cos(\varphi - \varphi') \sin\theta + h \cos\theta]} d\varphi' \quad (4a)$$

$$E_{c\varphi} = \frac{-j\omega\mu_0 a e^{-jk_0 r}}{4\pi r} \int_0^{2\pi} \cos(\varphi - \varphi') I(\varphi') e^{jk_0 [a \cos(\varphi - \varphi') \sin\theta + h \cos\theta]} d\varphi' \quad (4b)$$

for square loop: $\ell = s$

$$\begin{aligned}
 E_{s\theta} = & \frac{-j\omega\mu_0 e^{-jk_0 r} \cos\theta \sin\varphi}{4\pi r} \int_{-b/2}^{b/2} I(y') e^{jk_0 [y' \sin\varphi \sin\theta - \frac{b}{2} \cos\varphi \sin\theta + h \cos\theta]} dy' \\
 & + \frac{-j\omega\mu_0 e^{-jk_0 r} \cos\theta \cos\varphi}{4\pi r} \int_{-b/2}^{b/2} I(x') e^{jk_0 [x' \cos\varphi \sin\theta - \frac{b}{2} \sin\varphi \sin\theta + h \cos\theta]} dx' \\
 & + \frac{-j\omega\mu_0 e^{-jk_0 r} \cos\theta \sin\varphi}{4\pi r} \int_{b/2}^{-b/2} I(y') e^{jk_0 [y' \sin\varphi \sin\theta + \frac{b}{2} \cos\varphi \sin\theta + h \cos\theta]} dy' \\
 & + \frac{-j\omega\mu_0 e^{-jk_0 r} \cos\theta \cos\varphi}{4\pi r} \int_{b/2}^{-b/2} I(x') e^{jk_0 [x' \cos\varphi \sin\theta + \frac{b}{2} \sin\varphi \sin\theta + h \cos\theta]} dx' \quad (5a)
 \end{aligned}$$

$$\begin{aligned}
 E_{s\varphi} = & \frac{-j\omega\mu_0 e^{-jk_0 r} \cos\varphi}{4\pi r} \int_{-b/2}^{b/2} I(y') e^{jk_0 [y' \sin\varphi \sin\theta - \frac{b}{2} \cos\varphi \sin\theta + h \cos\theta]} dy' \\
 & + \frac{j\omega\mu_0 e^{-jk_0 r} \sin\varphi}{4\pi r} \int_{b/2}^{-b/2} I(x') e^{jk_0 [x' \cos\varphi \sin\theta - \frac{b}{2} \sin\varphi \sin\theta + h \cos\theta]} dx' \\
 & + \frac{-j\omega\mu_0 e^{-jk_0 r} \cos\varphi}{4\pi r} \int_{b/2}^{-b/2} I(y') e^{jk_0 [y' \sin\varphi \sin\theta + \frac{b}{2} \cos\varphi \sin\theta + h \cos\theta]} dy' \\
 & + \frac{j\omega\mu_0 e^{-jk_0 r} \sin\varphi}{4\pi r} \int_{-b/2}^{b/2} I(x') e^{jk_0 [x' \cos\varphi \sin\theta + \frac{b}{2} \sin\varphi \sin\theta + h \cos\theta]} dx' \quad (5b)
 \end{aligned}$$

It may be remarked that the respective currents carried by the wire elements (including the loop) are determined using the method of moments. The front-to-back ratio (F/B), is calculated here using the standard formula:

$$F/B \text{ (dB)} = 10 \log_{10} \left[\frac{|E_\theta(\theta_f, \varphi_f)|^2 + |E_\varphi(\theta_f, \varphi_f)|^2}{|E_\theta(\theta_b, \varphi_b)|^2 + |E_\varphi(\theta_b, \varphi_b)|^2} \right] \quad (5c)$$

where (θ_f, φ_f) and (θ_b, φ_b) assume the respective values $(0^\circ, 0^\circ)$ and $(180^\circ, 0^\circ)$. Expressions utilized for other antenna parameters remain the same as those described elsewhere, [1]. Some computational results based on the above equations will now be presented.

3. COMPUTATIONAL RESULTS

Computational results are obtained based on the following values of parameters featuring in the above equations: a centre frequency of 1.25 GHz; square loop perimeter of 1λ which corresponds to 0.25λ side-length, radius of circular loop = 0.141λ ; the side-length of the square ground plane is 1λ , divided into eight equal segments; the loop height above the plane ranges from 0.05λ to 1.00λ ; wire radius = 0.001λ . The circular loop is excited at $\varphi = 0^\circ$ by a 1 V delta-gap source while the square loop is similarly excited at the corner ($x = 0.125\lambda$ and $y = -0.125\lambda$). The discussion of results begins with the input impedance.

3.1. Input Impedance

The calculated values of input resistance R_{in} and input reactance X_{in} of the circular- and square loop antennas at various antenna heights from 0.05λ to 1.00λ are plotted in Figure 2. It is worth

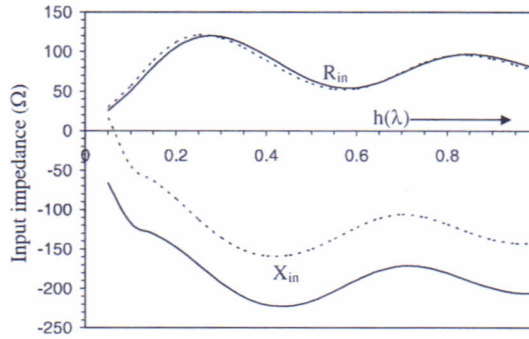


Figure 2: The input resistance R_{in} and input reactance X_{in} of the circular- and square-loop antennas versus the antenna height in wavelengths: —: circular loop; - - -: square loop.

reiterating that both loops are characterized by equal cross-sectional area. Evidently from the figure, one can see that both loops share virtually identical input resistance profiles, which vary in a sinusoidal fashion as the antenna height increases with the minimum R_{in} occurring at height 0.05λ . The variation of R_{in} from about $25\ \Omega$ to $125\ \Omega$ seems reasonable for some practical applications. On the other hand, there are marked differences in the input reactance X_{in} of circular loop and square loop even though the X_{in} profiles of both antenna appear similar. The square loop has input reactance values that are in general, lower than the input reactance of the circular loop for antenna height range $0.05\lambda \leq h \leq 1.00\lambda$ specified in this work. Remarkably, the square loop resonates at antenna height of 0.054λ while the circular loop does not, perhaps because of the corresponding lesser circumference of the circular loop which is 0.886λ .

3.2. Far-zone Electric Fields

Depicted in Figure 3 are the E_φ components of the radiated electric fields of the square- and circular-loop antennas superimposed on each other, on the E -plane ($\varphi = 0^\circ$) at various values of loop height. When the loops are at close proximity to the wire-grid ground plane (at $h = 0.05\lambda$), the major lobe is in the forward direction ($\theta = 0^\circ$), however, the back-lobe is appreciable which may be attributable to the strong interactions between the loops and the wire grids. As the antenna height increases, the magnitude of the back lobe decreases, and almost becomes negligible at loop height 0.30λ , with a well-defined major lobe in the forward direction. But at height 0.4λ , the direction of the major lobe shifts from the desired direction ($\theta = 0^\circ$) to a new direction $\theta = 35^\circ$, with a slight increase of the field component in the backward direction. Beyond $h = 0.40\lambda$, the patterns become more distorted and typified by side lobes as well as forward and backward lobes. It is noteworthy that at $h = 1.00\lambda$, the antenna patterns have no distinct well-formed lobes. To a large extent, the difference between the patterns of circular loop and square loop seems insignificant.

The E_θ components on the H -plane ($\varphi = 90^\circ$) of the radiated electric fields of the loop antennas at different loop heights from the wire-grid ground plane are graphically illustrated in Figure 4. As observed for the E_φ components above, the back lobe of the E_θ pattern at height 0.05λ is considerable due to aforementioned reason. However, as the antenna height increases, good reduction in the backlobe size is noted till the height is 0.30λ . Above loop height 0.30λ , the back-lobes begin to build up significantly as the loop height increases, although the back lobes at $h = 0.80\lambda$ are smaller than those at $h = 1.00\lambda$. It should be stated that at loop height 1.00λ , the E_θ patterns of both loops have degenerated into several lobes. Again, the E_θ patterns of both loops are somewhat indifferent.

From the features of E_θ and E_φ patterns in Figures 3 and 4, it is logical to limit the antenna height to a value less than 0.30λ .

3.3. Directive Gain and Front-to-Back Ratio (F/B)

To further illuminate the radiation characteristics of the circular- and square-loop antennas above a wire-grid plane of finite extent, the directive gain and front-to-back (F/B) of the radiation intensity of both loops are evaluated at several loop heights, and illustrated in the graphs displayed in Figures 5 and 6, respectively. It can be seen from Figure 5 that the forward directive gain G_d is maximum for both loops at height 0.05λ , and gradually decreases as the loop height increases. Worthy of note is the dip between heights 0.48λ and 0.57λ for both loops, and subsequent increase in G_d at height above 0.57λ . The G_d profiles in general exhibit the “notch filter response” behaviour

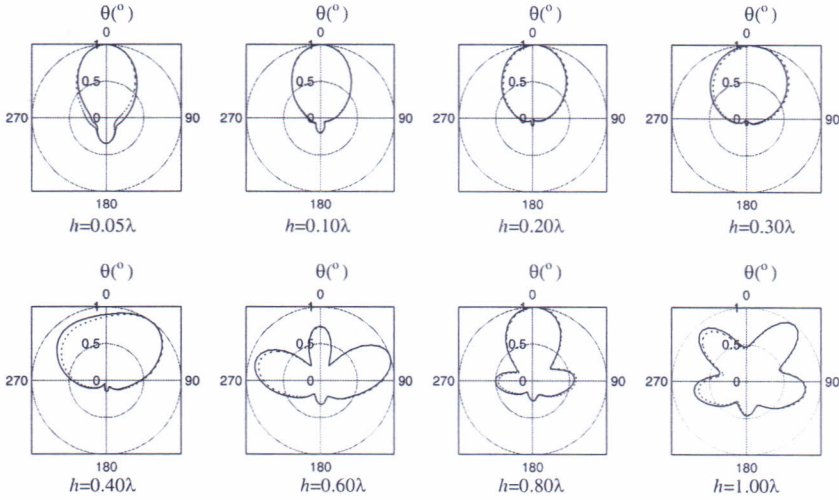


Figure 3: The E_φ components of the radiated fields on the E -plane ($\varphi = 0^\circ$) at various antenna heights: —: circular loop; - - -: square loop.

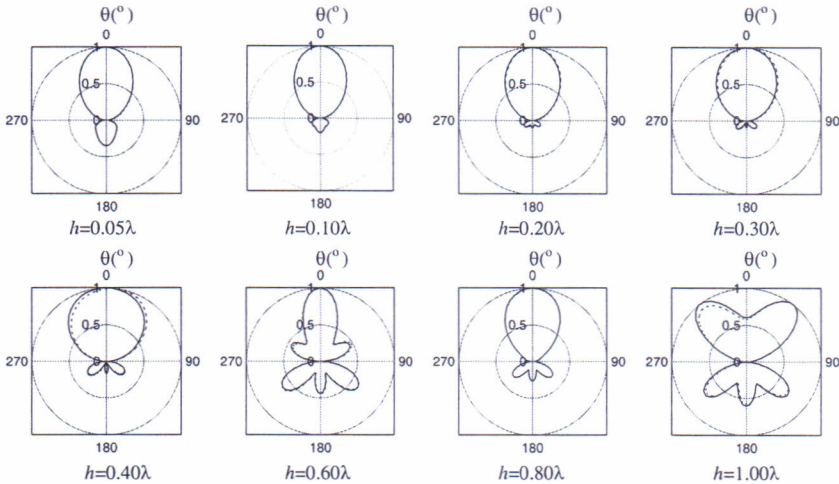


Figure 4: The E_θ components of the radiated fields on the H -plane ($\varphi = 90^\circ$) at different antenna heights: —: circular loop; - - -: square loop.

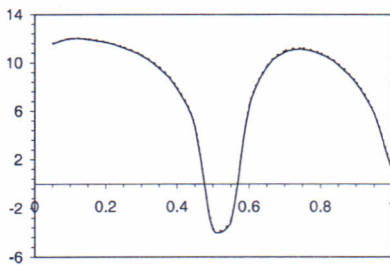


Figure 5: Forward directive gain G_d profiles of the circular- and square-loop antennas as a function of antenna height. —: circular loop; - - -: square loop.

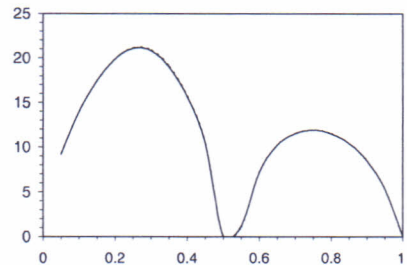


Figure 6: Variation of front-to-back ratio (F/B) of the radiation intensity of the circular- and square-loop antennas against the antenna height. —: circular loop; - - -: square .

which is consistent with the previous results of Hejase et al. [4] who employed the physical optics (PO) method to study similar problem.

The front-to-back ratio which gives a comparison between the radiation intensity in the forward

direction and backward direction, is shown in Figure 6 as a function of loop height. It is noted that the F/B is maximum at $h = 0.25\lambda$, which is in agreement with the E_θ and E_φ patterns. Lastly, the F/B profiles are the same for both loops, and they are in accordance with the G_d profiles.

4. CONCLUDING REMARKS

Using our previous formulation for loop antenna above ground plane of finite extent, modeled by wire grids, new results are obtained and reported here when the circular- and square-loop antennas have equal cross-sectional area, unlike in the prior presentation when the loops have equal perimeter of one wavelength. It is found that the loops have nearly identical input resistance profiles, whereas the input reactance values of the square loop are lower than those for the circular loop in the range of loop height specified. The radiation field patterns in the E - and H -planes suggest that the loop heights should be less than 0.3λ for well-defined major lobes in the forward direction, and negligible back-lobe. Finally, it is observed that the forward directive gain profile is identical to the “notch filter response” behavior.

REFERENCES

1. Ayorinde, A. A., S. A. Adekola, and A. I. Mowete, “Performance characteristics of loop antennas above a ground plane of finite extent,” *PIERS Proceedings*, 769–744, Taipei, March 25–28, 2013.
2. Rajarayamont, B. and T. Sekiguchi, “One-element loop antenna with finite reflector,” *Elect. & Comm. in Japan*, Vol. 59B, No. 5, 68–75, 1976.
3. Iwashige, J., “Analysis of loop antenna with circular reflector and its properties,” *Elect. & Comm. in Japan*, Vol. 63B, No. 11, 44–50, 1982.
4. Hejase, H., S. D. Gedney, and K. W. Whites, “Effect of a finite ground plane on radiated emissions from a circular loop antenna,” *IEEE Trans. Electromagnetic Comp.*, Vol. 36, No. 4, 364–371, 1994.
5. Shoamanesh, A. and L. Shafai, “Characteristics of circular loop antennas above a lossless ground plane,” *IEEE Trans. Ant. & Prop.*, Vol. 29, No. 3, 528–529, 1981.
6. Smith, G. S., “Loop antennas,” *Antenna Engineering Handbook*, Richard C. Johnson, Ed., 3rd Edition, Chapter 5, McGraw-Hill, 1984.
7. Harrington, R. F., “Matrix methods for field problems,” *Proc. IEEE*, Vol. 55, 136–149, 1967.